Computers and Mathematics with Applications

Manuscript Draft

Manuscript Number: CAMWA-D-17-01692

Title: A Two-grid Decoupled Algorithm for Fracture Models

Article Type: Regular Article

Keywords: Fracture model; two-grid method; Darcy's law; Darcy-Forcheimer's law; decoupling

Abstract: In this paper, we consider numerical methods for two categories of fracture models: Models coupling Darcy flow in the fracture and surrounding domains and those in which flow in the fracture is governed by Darcy-Forchheimer law and in the matrix is governed by Darcy law. We propose two-grid methods for decoupling the fractures and sub-domains by using the coarse grid approximations in the interfaces. Error estimates show that the H^1 semi-norm of pressure and the (L^2)^2 norm of velocity exhibit optimal convergence rates for the first kind of models. And numerical experiments show that the decoupled two-grid algorithm holds the same order accuracy as the coupled one, which conforms our theoretical analysis and the computation times of two-grid method are reduced greatly.

A Two-grid Decoupled Algorithm for Fracture Models

Shuangshuang Chen[1], Hongxing Rui[1,*]

[1] *School of Mathematics, Shandong University, Jinan, Shandong, 250100, China.*

Abstract. In this paper, we consider numerical methods for two categories of fracture models: Models coupling Darcy flow in the fracture and surrounding domains and those in which flow in the fracture is governed by Darcy-Forchheimer law and in the matrix is governed by Darcy law. We propose two-grid methods for decoupling the fractures and sub-domains by using the coarse grid approximations in the interfaces. Error estimates show that the H^1 semi-norm of pressure p and the $(L^2)^2$ norm of velocity $\mathbf{u}$ exhibit optimal convergence rates for the first kind of models. And numerical experiments show that the decoupled two-grid algorithm holds the same order accuracy as the coupled one, which conforms our theoretical analysis and the computation times of two-grid method are reduced greatly.

Key words: Fracture model; two-grid method; Darcy's law; Darcy-Forcheimer's law; decoupling

Mathematics Subject Classification(2010): 65N12; 65N15; 65N30

1 Introduction

In this paper, we consider a single phase fluid flow in porous media with fractures. The permeabilities in fractures are much higher or lower (due to crystalization) and there are also interactions between fractures and surrounding domains, so fractures play significant roles in fluid flow. But numerical methods of them are very complicated just because of the great change of fracture permeability with small domains. Fractures generally have at least one dimension with very smaller width, and then an idea treating fractures as $(n-1)$-dimensional interfaces in the n-dimensional porous media was proposed in [1] for high permeability fracture models. In [2], a model was presented to generalize the earlier models and it was improved to handle both large and small permeability of fractures. For models with more permeable fractures, the fluid tends to flow into fractures and along fractures. Fractures can be seen as fast pathways in this case. The normal component of the velocity should not be expected to be continuous across fractures. While for models with less permeable fractures, it is easy to verify that the fluid has a tendency to avoid fractures. Fractures act as geological barriers. The pressure need not be identical on both sides of fractures. Hence, the fracture model in [2] coupled a flow equation along the fracture with equations in the surrounding domains without nonstandard Robin type conditions in the interface. And the interaction between fracture and matrix was also taken into account. We also refer to [3–6] for similar models. For

The work of second author is supported by the National Natural Science Foundation of China Grant (No. 91330106 , 11671233)

*Corresponding author: hxrui@sdu.edu.cn.

all of the above models, the linear Darcy's law is used as the constitutive law for flow in the fractures as well as in the surrounding domains. However, for high-ranged velocity, Darcy's law cannot fit well with experiments and a nonlinear correction term should be added, the Forchheimer term [7, 8]. For fractures with large enough permeability, the Darcy's law will be replaced by the Darcy-Forchheimer's law. A model coupling Darcy-Forchheimer flow in the fracture and Darcy's flow in the rest of the domain was carried out in [9], but the pressure was assumed to be continuous in this model. In [10](2014), a similar model without the continuity was derived, and the existence and uniqueness of the mixed finite element approximation was analyzed. In this paper, we consider a two-grid method using the coarse grid values in the interface to decouple the above mentioned fracture models in [2] and [10]. The decoupled local problems can be solved individually, and even on parallel processors, which is efficient and convenient.

The fracture model is one of multi-modeling problems consisting of multiple equations in different regions coupled via interface conditions. Most researches consider approaches solving the coupled model directly. However, different models defined in different regions are varied in type, such as coupling linear and nonlinear systems, and coupling interface conditions include variables in different domains, which results in very complex structures and numerical difficulties. Another approach is to decouple multi-modeling problems firstly, and then solve local models. There are some famous decoupling methods for domain decomposition, for example, Quarteroni and Valli [11], Lagrange multiplier techniques [12], and so on. In [13] and [14], Xu proposed a new two-grid discretization technique for solving partial differential equations. Then in [15] and [16], the two-grid method was successfully applied to decouple multi-modeling problem, and the mixed Stokes/Darcy and mixed Navier-Stokes/Darcy models were solved in the two articles, respectively.

In this paper, we will apply the two-grid decoupled method to fracture models. The basic idea of the algorithm is to use the coarse space to produce rough approximations of variables defined in the interface, and then the mixed models is decoupled to local problems, so this procedure is consist of a coupled solver on the coarse grid and a decoupled local solver in the fine grid. It is obvious that the two-grid decoupled algorithm is more flexible and convenient. The decoupled local algebraic systems are much simpler, and local problems can be solved by using suitable solvers individually, and even in a parallel multiprocess, so the computation times can be reduced greatly. Especially for the considered mixed Darcy-Forchheimer/Darcy model, the system in the fracture is nonlinear. If the decoupled method is applied, we just need to do iterations in the fracture instead of in the whole domain. More details about the two-grid method can be seen in [17–19]. The rest of this paper is organized as follows. In section 2, the coupled Darcy flow in both the fracture and surrounding media model is described and some notations and finite element spaces are introduced. The two-grid decoupled algorithm using a coarse grid approximation in the interface is proposed for the linear fracture model in Section 3. Error estimates for the two-grid method is discussed in Section 4. In Section 5, we extend the two-grid decoupled algorithm to the nonlinear system. The model coupling Darcy-Forchheimer flow in the fracture and Darcy flow in the matrix is considered. Finally, in Section 6, numerical experiments for the linear and nonlinear systems are carried out. And results show that the two-grid decoupled algorithm exhibits the same accuracy as the coupled method for pressure and velocity, which conforms our analysis, and decoupled method reduces computing time greatly. Hence, both theoretical analysis and numerical examples reveal the accuracy and efficiency of the proposed two-grid method.

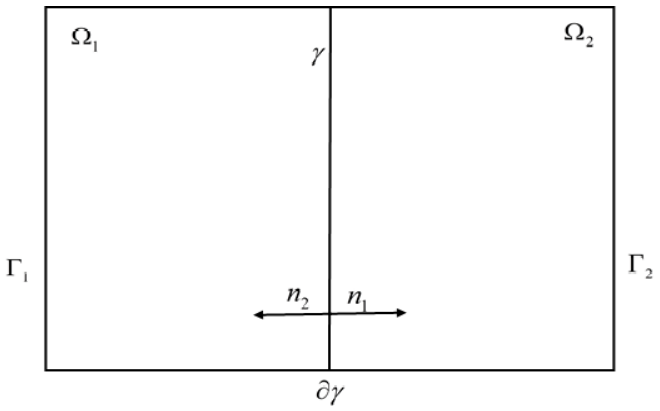

Figure 1: The domain of the fracture model

2 Description of the Problem and Notation

We firstly consider the fracture model described in [2], which couples 2-dimensional linear elliptic equations in surrounding domains with a 1-dimensional linear elliptic equation in the fracture. Let $\Omega = [a, b] \times [c, d]$ be a rectangle domain in $\mathbb{R}^2$ with the boundary Γ and let $\gamma = \{x = x_f\} \times [c, d] \subset \Omega$ be a one-dimensional surface as shown in Figure 1. Ω is separated by γ into two bounded subdomains:

$$\Omega_1 = [a, x_f) \times [c, d], \text{ and } \Omega_2 = (x_f, b] \times [c, d],$$
$$\Omega \subset \mathbb{R}^2, \ \Omega \backslash \gamma = \Omega_1 \cup \Omega_2, \ \Gamma = \partial\Omega.$$

Denote by Γ_i the part of the boundary of Ω_i in common with the boundary of Ω, $\Gamma_i = \partial\Omega_i \cap \Gamma$, $i = 1, 2$. We define the velocity and pressure on $\Omega_i, i = 1, 2$ and γ by $\mathbf{u}_i, p_i$ and u_f, p_f, respectively. We consider the following fracture problem, in which the flow in both the fracture and the surrounding matrix is governed by Darcy law together with the conservation property.

$$\begin{aligned}
\mathbf{u}_i &= -\mathbf{K}_i \nabla p_i && \text{in } \Omega_i, && i = 1, 2, \\
\text{div } \mathbf{u}_i &= q_i && \text{in } \Omega_i, && i = 1, 2, \\
u_f &= -k_{f,y} d \frac{\partial p_f}{\partial y} && \text{in } \gamma, && \\
\frac{\partial u_f}{\partial y} &= q_f + (\mathbf{u}_1 \cdot \mathbf{n}_1|_\gamma + \mathbf{u}_2 \cdot \mathbf{n}_2|_\gamma) && \text{in } \gamma, && \\
-\xi \mathbf{u}_i \cdot \mathbf{n}_i + \alpha_f p_i &= \alpha_f p_f - (1 - \xi) \mathbf{u}_{i+1} \cdot \mathbf{n}_{i+1} && \text{in } \gamma, && \\
p_i &= \bar{p}_i && \text{on } \Gamma_i, && i = 1, 2, \\
p_f &= \bar{p}_f && \text{on } \partial\gamma, &&
\end{aligned} \tag{2.1}$$

where $\mathbf{n}_i$ is the unit normal vector on the interface γ directed outward from Ω_i, $\mathbf{n}_1 = -\mathbf{n}_2$. In this paper, we assume that $\mathbf{K}_i, i = 1, 2, \mathbf{K}_f = \text{diag}(k_{f,x}, k_{f,y})$ are symmetric matrices representing the permeability of flow in $\Omega_i, i = 1, 2$ and γ, and there exist $k_{\max} > k_{\min} > 0$ such that

$$k_{\min}|\zeta|^2 \le \zeta \cdot \mathbf{K}_i \zeta \le k_{\max}|\zeta|^2, \quad \forall \zeta \in \mathbb{R}^2,$$

$$k_{\min} \le (k_{f,y} d), \ (k_{f,x}/d) \le k_{\max}.$$

The parameter d denotes the thickness of the fracture, the coefficient $\alpha_f = 2k_{f,x}/d$, and the constant $\xi \in (1/2, 1]$. The index i varies in $\mathbb{Z}/2\mathbb{Z}$ satisfying $2 + 1 = 1$.

Similar to [2], the Robin boundary conditions, the fifth equation in (2.1), can be rewritten as follows,

$$\begin{aligned} \mathbf{u}_2 \cdot \mathbf{n}_2|_\gamma + \mathbf{u}_1 \cdot \mathbf{n}_1|_\gamma &= \frac{\alpha_f}{2\xi - 1}(p_2|_\gamma + p_1|_\gamma - 2p_f), \\ \mathbf{u}_2 \cdot \mathbf{n}_2|_\gamma - \mathbf{u}_1 \cdot \mathbf{n}_1|_\gamma &= \alpha_f(p_2|_\gamma - p_1|_\gamma). \end{aligned} \tag{2.2}$$

Furthermore, we can obtain,

$$\mathbf{u}_i \cdot \mathbf{n}_i|_\gamma = \frac{\alpha_f}{2\xi - 1}(\xi p_i|_\gamma + (1-\xi)p_{i+1}|_\gamma - p_f), \quad i = 1, 2. \tag{2.3}$$

For simplicity, we suppose that α_f is constant, and we will consider the homogenous boundary conditions on p in the following analysis, i.e., $\bar{p}_i = 0$ and $\bar{p}_f = 0$, and the non-homogenous case can be handled by a lifting function. For any non-negative integer m and number $s \geq 1$, denote by $W^{m,s}$ the classical Sobolev space, equipped with the standard semi-norm $|\cdot|_{W^{m,s}}$ and norm $\|\cdot\|_{W^{m,s}}$. When $s = 2$, this is the Hilbert space H^m. We introduce the following finite element spaces.

$$\begin{aligned} W_i &= \{w_i \in H^1(\Omega_i) |\ w_i = 0, \text{ on } \Gamma_i\}, \quad i = 1, 2, \\ W_f &= \{w_f \in H^1(\gamma) |\ w_f = 0, \text{ on } \partial\gamma\}, \\ W &= \{w = (w_1, w_2, w_f) \in W_1 \times W_2 \times W_f\}, \end{aligned} \tag{2.4}$$

with the following norm

$$\|p\|_W = \sum_{i=1,2} \|p_i\|_{H^1(\Omega_i)} + \|p_f\|_{H^1(\gamma)}.$$

$$|p|_W = \sum_{i=1,2} |p_i|_{H^1(\Omega_i)} + |p_f|_{H^1(\gamma)}.$$

The weak formulation of the fracture model (2.1) can be written as follows: Find $p = (p_1, p_2, p_f) \in W$ such that

$$a(p, w) = \sum_{i=1,2} (q_i, w_i)_{\Omega_i} + (q_f, w_f)_\gamma, \quad \forall w = (w_1, w_2, w_f) \in W, \tag{2.5}$$

where $a(\cdot, \cdot)$ is the bilinear form from $W \times W$ to R

$$\begin{aligned} a(p, w) &= \sum_{i=1,2} (\mathbf{K}_i \nabla p_i, \nabla w_i)_{\Omega_i} + \left(k_{f,y} d \frac{\partial p_f}{\partial y}, \frac{\partial w_f}{\partial y} \right)_\gamma \\ &\quad + \sum_{i=1,2} \left(\frac{\alpha_f}{2\xi - 1}(\xi p_i + (1-\xi)p_{i+1} - p_f), w_i \right)_\gamma - \left(\frac{\alpha_f}{2\xi - 1}(p_1 + p_2 - 2p_f), w_f \right)_\gamma. \end{aligned} \tag{2.6}$$

It is easy to check the continuity of the bilinear form $a(\cdot, \cdot)$ over $W \times W$, and then we will verify that a is W-elliptic. Under the assumption of the permeability $\mathbf{K}_i$ and $\mathbf{K}_f$, for any $w = (w_1, w_2, w_f) \in W$,

$$\begin{aligned} a(w, w) &= \sum_{i=1,2} (\mathbf{K}_i \nabla w_i, \nabla w_i)_{\Omega_i} + \left(k_{f,y} d \frac{\partial w_f}{\partial y}, \frac{\partial w_f}{\partial y} \right)_\gamma \\ &\quad + \sum_{i=1,2} \frac{\alpha_f}{2\xi - 1} \left(\xi w_i + (1-\xi) w_{i+1} - w_f, w_i - w_f \right)_\gamma. \end{aligned}$$

Since

$$\begin{aligned}
&\sum_{i=1,2} (\xi w_i + (1-\xi) w_{i+1} - w_f, w_i - w_f)_\gamma \\
= &\sum_{i=1,2} (\xi(w_i - w_f) + (1-\xi)(w_{i+1} - w_f), w_i - w_f)_\gamma \\
= &\ \xi \sum_{i=1,2} (w_i - w_f, w_i - w_f)_\gamma - 2(1-\xi)(w_1 - w_f, w_2 - w_f)_\gamma \\
\geq &\ (2\xi - 1) \sum_{i=1,2} \|w_i - w_f\|^2_{L^2(\gamma)}.
\end{aligned}$$

We get

$$a(w,w) \geq k_{\min} \left(\sum_{i=1,2} |w_i|^2_{H^1(\Omega_i)} + |w_f|^2_{H^1(\gamma)} \right) + \alpha_f \sum_{i=1,2} \|w_i - w_f\|^2_{L^2(\gamma)}.$$

And by the Poincare inequality,

$$\sum_{i=1,2} \|w_i\|_{L^2(\Omega_i)} + \|w_f\|_{L^2(\gamma)} \leq \sum_{i=1,2} C(|w_i|_{H^1(\Omega_i)} + |w_f|_{H^1(\gamma)}).$$

There exists a constant c satisfying

$$a(w,w) \geq c \left(\sum_{i=1,2} \|w_i\|^2_{H^1(\Omega_i)} + \|w_f\|^2_{H^1(\gamma)} + \sum_{i=1,2} \|w_i - w_f\|^2_{L^2(\gamma)} \right).$$

Hence, the model problem has a unique solution.

3 The two-grid algorithm for the fracture model

Suppose that $\mathcal{T}_i^h$ is a triangulation of the sub-domain $\Omega_i, i = 1, 2$ with the longest diameter of elements h_i. And $\mathcal{T}_1^h$ and $\mathcal{T}_2^h$ align in the fracture γ to form a partition of γ,

$$\mathcal{T}_f^h : \ c = y_0 < y_1 < \cdots < y_n = d.$$

Define

$$y_{\ell+1/2} = \frac{y_\ell + y_{\ell+1}}{2}, \quad \text{and} \quad \sigma_{\ell+1/2} = (y_\ell, y_{\ell+1}), \quad \ell = 0, \cdots, n-1.$$

Define $\mathcal{T}^h = \cup_{i=1,2} \mathcal{T}_i^h \cup \mathcal{T}_f^h$ with $h = \max_{i=1,2} h_i$. For the fracture model (2.1), we consider the conforming linear finite element space $W^h = W_1^h \times W_2^h \times W_f^h$ defined on $\mathcal{T}^h$. For $i = 1, 2$, $W_i^h \subset W_i$,

$$W_i^h = \left\{ w_i^h \in H^1(\Omega) : w_i^h \text{ is linear for any } K \in \mathcal{T}_h^i, \ w_i^h = 0, \text{ on } \partial\Omega \right\}.$$

And $W_f^h \subset W_f$,

$$W_f^h = \left\{ w_f^h \in H^1(\gamma) : w_f^h \text{ is linear in any } \sigma_{\ell+1/2}, \ell = 0, \cdots, n-1, \ w_f^h = 0, \text{ on } \partial\gamma \right\}.$$

The coupled finite element discretization for the fracture model reads as follows.

Algorithm 1. Find $p^h = (p_1^h, p_2^h, p_f^h) \in W^h$ such that

$$a(p^h, w^h) = \sum_{i=1,2} (q_i, w_i^h)_{\Omega_i} + (q_f, w_f^h)_\gamma, \quad \forall w^h = (w_1^h, w_2^h, w_f^h) \in W^h. \tag{3.1}$$

We then propose a two-grid algorithm for decoupling the fracture model using a coarse grid approximation in the interface.

Algorithm 2.

1. Solve a coarse grid coupled problem: Find $p^H = (p_1^H, p_2^H, p_f^H) \in W^H$ such that

$$a(p^H, w^H) = \sum_{i=1,2} (q_i, w_i^H)_{\Omega_i} + (q_f, w_f^H)_\gamma, \quad \forall w^H = (w_1^H, w_2^H, w_f^H) \in W^H. \tag{3.2}$$

2. Solve a decoupled fine grid problem: Find $\hat{p}^h = (\hat{p}_1^h, \hat{p}_2^h, \hat{p}_f^h) \in W^h$ satisfying for any $w^h = (w_1^h, w_2^h, w_f^h) \in W^h$,

$$\begin{aligned} & \sum_{i=1,2} (\mathbf{K}_i \nabla \hat{p}_i^h, \nabla w_i^h)_{\Omega_i} + \left(k_{f,y} d \frac{\partial \hat{p}_f^h}{\partial y}, \frac{\partial w_f^h}{\partial y} \right)_\gamma + \sum_{i=1,2} \frac{\alpha_f}{2\xi - 1} \left(\xi \hat{p}_i^h, w_i^h \right)_\gamma + \frac{\alpha_f}{2\xi - 1} \left(2\hat{p}_f^h, w_f^h \right)_\gamma \\ = & -\sum_{i=1,2} \frac{\alpha_f}{2\xi - 1} \left((1-\xi) p_{i+1}^H, w_i^h \right)_\gamma + \sum_{i=1,2} \frac{\alpha_f}{2\xi - 1} \left((1-\xi) p_f^H, w_i^h \right)_\gamma + \sum_{i=1,2} \frac{\alpha_f}{2\xi - 1} \left(p_i^H, w_f^h \right)_\gamma \\ & + \sum_{i=1,2} (q_i, w_i^h)_{\Omega_i} + (q_f, w_f^h)_\gamma. \end{aligned} \tag{3.3}$$

We can easily check that the decoupled fine grid problem is well-posed and it is equivalent to three local problems defined on three sub-domains Ω_1, Ω_2 and γ.

The discrete Darcy problem defined in the matrix $\Omega_i, i = 1, 2$:

$$(\mathbf{K}_i \nabla \hat{p}_i^h, \nabla w_i^h)_{\Omega_i} + \frac{\alpha_f}{2\xi - 1} \left(\xi \hat{p}_i^h, w_i^h \right)_\gamma = -\frac{\alpha_f}{2\xi - 1} \left((1-\xi) p_{i+1}^H, w_i^h \right)_\gamma + \frac{\alpha_f}{2\xi - 1} \left(p_f^H, w_i^h \right)_\gamma + (q_i, w_i^h)_{\Omega_i}. \tag{3.4}$$

The discrete Darcy problem defined in the fracture γ:

$$\left(k_{f,y} d \frac{\partial \hat{p}_f^h}{\partial y}, \frac{\partial w_f^h}{\partial y} \right)_\gamma + \frac{\alpha_f}{2\xi - 1} \left(2\hat{p}_f^h, w_f^h \right)_\gamma = \sum_{i=1,2} \frac{\alpha_f}{2\xi - 1} \left(p_i^H, w_f^h \right)_\gamma + (q_f, w_f^h)_\gamma. \tag{3.5}$$

4 Error estimate

Theorem 4.1 *For the coupled method Algorithm 1, we suppose that exact solutions $p_i \in H^2(\Omega_i), i = 1, 2$, and $p_f \in H^2(\gamma)$, then the following error estimates hold.*

$$\begin{aligned} & \sum_{i=1,2} |p_i - p_i^h|_{H^1(\Omega_i)} + |p_f - p_f^h|_{H^1(\gamma)} \le Ch, \\ & \sum_{i=1,2} \|p_i - p_i^h\|_{L^2(\Omega_i)} + \|p_f - p_f^h\|_{L^2(\gamma)} \le Ch^2. \end{aligned} \tag{4.1}$$

Proof. Subtracting the discrete model (3.1) from (2.5), we get

$$a(p-p^h, w^h) = 0, \quad \forall w^h \in W^h. \tag{4.2}$$

Let $p^I = (p_1^I, p_2^I, p_f^I) \in W^h$ be the orthogonal L^2 projection satisfying

$$\int_{\Omega_i} (p_i^I - p_i) w_i d\mathbf{x} = 0, \quad \forall w_i \in W_i^h, \quad i = 1, 2,$$

$$\int_{\gamma} (p_f^I - p_f) w_f ds = 0, \quad \forall w_f \in W_f^h,$$

with the following properties

$$\begin{aligned} &h|p_i^I - p_i|_{W^{1,s}(\Omega_i)} + \|p_i^I - p_i\|_{L^s(\Omega_i)} \le Ch^2 \|p_i\|_{W^{2,s}(\Omega_i)}, \quad i = 1, 2, \\ &h|p_f^I - p_f|_{W^{1,s}(\gamma)} + \|p_f^I - p_f\|_{L^s(\gamma)} \le Ch^2 \|p_f\|_{W^{2,s}(\gamma)}. \end{aligned}$$

In (4.2), taking $w^h = p^h - p^I \in W^h$, we obtain

$$a(p^I - p^h, p^I - p^h) = -a(p - p^I, p^I - p^h).$$

Since $a(\cdot, \cdot)$ is coercive and continuity over W,

$$\begin{aligned} & \left(\sum_{i=1,2} |p_i^I - p_i^h|_{H^1(\Omega_i)}^2 + |p_f^I - p_f^h|_{H^1(\gamma)}^2 + \sum_{i=1,2} \|(p_i^I - p_i^h) - (p_f^I - p_f^h)\|_{L^2(\gamma)}^2 \right)^{1/2} \\ \le \; & C \left(\sum_{i=1,2} |p_i^I - p_i^h|_{H^1(\Omega_i)} + |p_f^I - p_f^h|_{H^1(\gamma)} + \sum_{i=1,2} \|(p_i^I - p_i^h) - (p_f^I - p_f^h)\|_{L^2(\gamma)} \right) \\ \le \; & Ch. \end{aligned}$$

And by the properties of the projection p^I, the error estimate for the H^1 semi-norm holds.

We turn our attention to the estimate for the L^2 norm. Using the Aubin-Nitsche duality technique [20], we consider the following dual problem defined by the error $p - p^h$,

$$a(v, w) = \sum_{i=1,2} (p_i - p_i^h, w_i)_{\Omega_i} + (p_f - p_f^h, w_f)_{\gamma}, \quad \forall w = (w_1, w_2, w_f) \in W. \tag{4.3}$$

We assume that $v = (v_1, v_2, v_f) \in H^2(\Omega_1) \times H^2(\Omega_2) \times H^2(\gamma)$ is the solution to the dual problem, and

$$\sum_{i=1,2} \|v_i\|_{H^2(\Omega_i)} + \|v_f\|_{H^2(\gamma)} \le C \left(\sum_{i=1,2} \|p_i - p_i^h\|_{L^2(\Omega_i)} + \|p_f - p_f^h\|_{L^2(\gamma)} \right). \tag{4.4}$$

Taking $w = p - p^h$ in (4.3),

$$a(v, p - p^h) = \sum_{i=1,2} (p_i - p_i^h, p_i - p_i^h)_{\Omega_i} + (p_f - p_f^h, p_f - p_f^h)_{\gamma}.$$

And Comparing (2.5) and (3.1), we have

$$a(p - p^h, v^h) = 0, \quad \forall v^h \in W^h.$$

Hence,

$$\begin{aligned}
&\sum_{i=1,2} \|p_i - p_i^h\|^2_{L^2(\Omega_i)} + \|p_f - p_f^h\|^2_{L^2(\gamma)} \\
= \;& a(p - p^h, v - v^h) \\
\leq \;& \left(\sum_{i=1,2} |p_i - p_i^h|_{H^1(\Omega_i)} + |p_f - p_f^h|_{H^1(\gamma)} + \sum_{i=1,2} \|(p_i - p_i^h) - (p_f - p_f^h)\|_{L^2(\gamma)} \right) \\
& \left(\sum_{i=1,2} |v_i - v_i^h|_{H^1(\Omega_i)} + |v_f - v_f^h|_{H^1(\gamma)} + \sum_{i=1,2} \|(v_i - v_i^h) - (v_f - v_f^h)\|_{L^2(\gamma)} \right) \\
\leq \;& Ch^2 \left(\sum_{i=1,2} \|v_i\|_{H^2(\Omega_i)} + \|v_f\|_{H^2(\gamma)} \right) \leq Ch^2 \left(\sum_{i=1,2} \|p_i - p_i^h\|_{L^2(\Omega_i)} + \|p_f - p_f^h\|_{L^2(\gamma)} \right).
\end{aligned} \tag{4.5}$$

The result holds.

□

We can immediately obtain the following estimates by Theorem 4.1

$$\begin{aligned}
&\sum_{i=1,2} |p_i^h - p_i^H|_{H^1(\Omega_i)} + |p_f^h - p_f^H|_{H^1(\gamma)} \leq CH, \\
&\sum_{i=1,2} \|p_i^h - p_i^H\|_{L^2(\Omega_i)} + \|p_f^h - p_f^H\|_{L^2(\gamma)} \leq CH^2.
\end{aligned} \tag{4.6}$$

Theorem 4.2 *Let $p^h = (p_1^h, p_2^h, p_f^h)$ and $\hat{p}^h = (\hat{p}_1^h, \hat{p}_2^h, \hat{p}_f^h)$ be solutions to the coupled method Algorithm 1 and two-grid decoupled method Algorithm 2, respectively. The following error estimate holds.*

$$\sum_{i=1,2} |p_i^h - \hat{p}_i^h|_{H^1(\Omega_i)} + |p_f^h - \hat{p}_f^h|_{H^1(\gamma)} \leq CH^{3/2}.$$

Proof. Subtracting the discrete decoupled problem (3.3) form the discrete coupled one (3.1), yields

$$\begin{aligned}
&\sum_{i=1,2} (\mathbf{K}_i \nabla(p_i^h - \hat{p}_i^h), \nabla w_i^h)_{\Omega_i} + \left(k_{f,y} d \frac{\partial(p_f^h - \hat{p}_f^h)}{\partial y}, \frac{\partial w_f^h}{\partial y} \right)_\gamma + \sum_{i=1,2} \frac{\alpha_f}{2\xi - 1} \left(\xi(p_i^h - \hat{p}_i^h), w_i^h \right)_\gamma \\
&+ \frac{\alpha_f}{2\xi - 1} \left(2(p_f^h - \hat{p}_f^h), w_f^h \right)_\gamma \\
= \;& - \sum_{i=1,2} \frac{\alpha_f}{2\xi - 1} \left((1 - \xi)(p_i^h - p_{i+1}^H), w_i^h \right)_\gamma + \sum_{i=1,2} \frac{\alpha_f}{2\xi - 1} \left((1 - \xi)(p_f^h - p_f^H), w_i^h \right)_\gamma \\
&+ \sum_{i=1,2} \frac{\alpha_f}{2\xi - 1} \left((p_i^h - p_i^H), w_f^h \right)_\gamma.
\end{aligned} \tag{4.7}$$

In the above equation, taking $w^h = (w_1^h, w_2^h, w_f^h) = (p_1^h - \hat{p}_1^h, p_2^h - \hat{p}_2^h, p_f^h - \hat{p}_f^h) \in W^h$, we get

$$\begin{aligned}
& k_{\min}\left(\sum_{i=1,2}|p_i^h-\hat{p}_i^h|^2_{H^1(\Omega_i)}+|p_f^h-\hat{p}_f^h|^2_{H^1(\gamma)}\right)+\sum_{i=1,2}\frac{\alpha_f\xi}{2\xi-1}\|p_i^h-\hat{p}_i^h\|^2_{L^2(\gamma)}+\frac{2\alpha_f}{2\xi-1}\|p_f^h-\hat{p}_f^h\|^2_{L^2(\gamma)}\\
\leq\ & \sum_{i=1,2}\frac{\alpha_f(1-\xi)}{2\xi-1}\|p_i^h-p_{i+1}^H\|_{L^2(\gamma)}\|p_i^h-\hat{p}_i^h\|_{L^2(\gamma)}+\sum_{i=1,2}\frac{\alpha_f(1-\xi)}{2\xi-1}\|p_f^h-p_f^H\|_{L^2(\gamma)}\|p_i^h-\hat{p}_i^h\|_{L^2(\gamma)}\\
& +\sum_{i=1,2}\frac{\alpha_f}{2\xi-1}\|p_i^h-p_i^H\|_{L^2(\gamma)}\|p_f^h-\hat{p}_i^f\|_{L^2(\gamma)}\\
\leq\ & \frac{k_{\min}}{2}\left(\sum_{i=1,2}\|p_i^h-\hat{p}_i^h\|^2_{L^2(\gamma)}+\|p_f^h-\hat{p}_f^h\|^2_{L^2(\gamma)}\right)+C\left(\sum_{i=1,2}\|p_i^h-p_i^H\|^2_{L^2(\gamma)}+\|p_f^h-p_f^H\|^2_{L^2(\gamma)}\right).
\end{aligned} \tag{4.8}$$

Thanks to $\|p_i^h - p_i^H\|_{L^2(\gamma)} \leq CH^{3/2}$,

$$\sum_{i=1,2}|p_i^h-\hat{p}_i^h|_{H^1(\Omega_i)}+|p_f^h-\hat{p}_f^h|_{H^1(\gamma)}+\sum_{i=1,2}\|p_i^h-\hat{p}_i^h\|_{L^2(\gamma)}+\|p_f^h-\hat{p}_f^h\|_{L^2(\gamma)}\leq CH^{3/2}. \tag{4.9}$$

□

Remark 4.1 *Together with Theorem 4.1, we can immediately get the following error estimate between the exact solution p and the two-grid decoupled finite element approximation $\hat{p}^h$.*

$$\sum_{i=1,2}|p_i-\hat{p}_i^h|_{H^1(\Omega_i)}+|p_f-\hat{p}_f^h|_{H^1(\gamma)}\leq Ch+CH^{3/2}.$$

If $h = H^{3/2}$, Theorem 4.2 shows that the numerical approximation of the decoupled two-grid algorithm holds an optical convergence rate $O(h)$ for the H^1 semi-norm of the pressure. Therefore, the fracture model is efficiently decoupled by the proposed two-grid method using values of the coarse grid in the interface. The decoupled local problems can be solved independently and they can be complemented on a parallel processes, which is efficient and flexible.

5 Nonlinear system

In this section, we consider a fracture model coupling Darcy flow in the matrix and Darcy-Forchheimer flow in the fracture derived in [9, 10]. In fracture media, when the permeability is much greater than the surrounding domains, the flow rate in the fracture is very high. And in this case, experiments show that a nonlinear correction, the Forchheimer term, need be added in the fracture. Then the fracture model combining Darcy flow in surrounding matrix and Darcy-Forchheimer flow in the fracture fits well. The detailed description of this nonlinear system is written as follows.

$$\begin{aligned}
\alpha_i\mathbf{u}_i+\nabla p_i &= 0 && \text{in } \Omega_i, && i=1,2,\\
\operatorname{div}\mathbf{u}_i &= q_i && \text{in } \Omega_i, && i=1,2,\\
p_i &= \bar{p}_i && \text{on } \Gamma_i, && i=1,2,\\
(\alpha_\gamma+\beta_\gamma|u_f|)u_f+\frac{\partial p_f}{\partial y} &= g && \text{in } \gamma, &&\\
\frac{\partial u_f}{\partial y} &= q_f+(\mathbf{u}_1\cdot\mathbf{n}_1|_\gamma+\mathbf{u}_2\cdot\mathbf{n}_2|_\gamma) && \text{in } \gamma, &&\\
p_f &= \bar{p}_f && \text{on } \partial\gamma, &&
\end{aligned} \tag{5.1}$$

and the interface condition

$$p_i \;=\; p_f + \kappa\,(\mathbf{u}_i\cdot\mathbf{n}_i - (1-\xi)\mathbf{u}_{i+1}\cdot\mathbf{n}_{i+1}) \quad \text{in} \quad \gamma, \qquad i=1,2, \tag{5.2}$$

where $\alpha_i,\ i=1,2$, and α_γ are related to the inverse of the permeability on the sub-domains $\Omega_i,\ i=1,2$, and γ, respectively, and β_γ is the Forchheimer coefficient, and κ defined in γ is the coefficient scalar function related to the fracture width and inversely to the normal component of the permeability in the fracture. In this paper, we suppose that α_i is symmetric matrix and positive defined

$$\begin{array}{rcccl} \underline{\alpha_i}|\zeta|^2 & \le & \zeta\cdot\alpha_i\zeta & \le & \bar{\alpha}_i|\zeta|^2, \quad \forall\zeta\in\mathbb{R}^2,\\ \underline{\alpha}_\gamma & \le & \alpha_\gamma & \le & \bar{\alpha}_\gamma,\\ \underline{\beta}_\gamma & \le & \beta_\gamma & \le & \bar{\beta}_\gamma,\\ \underline{\kappa} & \le & \kappa & \le & \bar{\kappa}. \end{array}$$

Similar to [21], for the Darcy-Forchheimer equation in the fracture, the flux u_f can be rewritten as follows by expressing the term $|u_f|$,

$$u_f = -\frac{2}{\alpha_\gamma + \sqrt{\alpha_\gamma^2 + 4\beta_\gamma|\frac{\partial p_f}{\partial y} - g|}}\left(\frac{\partial p_f}{\partial y} - g\right).$$

And for the Robin boundary condition in the interface,

$$\mathbf{u}_2\cdot\mathbf{n}_2|_\gamma + \mathbf{u}_1\cdot\mathbf{n}_1|_\gamma = \frac{1}{(2\xi-1)\kappa}(p_2|_\gamma + p_1|_\gamma - 2p_f).$$

Then the system of flow in the fracture is described as follows.

$$-\frac{\partial}{\partial y}\left(\frac{2\left(\frac{\partial p_f}{\partial y} - g\right)}{\alpha_\gamma + \sqrt{\alpha_\gamma^2 + 4\beta_\gamma|\frac{\partial p_f}{\partial y} - g|}}\right) = q_f + \frac{1}{(2\xi-1)\kappa}(p_2|_\gamma + p_1|_\gamma - 2p_f), \quad \text{in } \gamma. \tag{5.3}$$

For simplicity, we assume that $g=0$ in our analysis. And denote by W the finite element method as follows.

$$\begin{array}{rcl} W_i & = & \{w_i\in H^1(\Omega_i)|\ w_i = 0,\ \text{on } \Gamma_i\}, \quad i=1,2,\\ W_f & = & \{w_f\in W^{1,3/2}(\gamma)\cap L^2(\gamma)|\ w_f = 0,\ \text{on } \partial\gamma\},\\ W & = & \{w=(w_1,w_2,w_f)\in W_1\times W_2\times W_f\}, \end{array} \tag{5.4}$$

with the following norm

$$\|p\|_W = \sum_{i=1,2}\|p_i\|_{H^1(\Omega_i)} + \|p_f\|_{W^{1,3/2}(\gamma)},$$

$$|p|_W = \sum_{i=1,2}|p_i|_{H^1(\Omega_i)} + |p_f|_{W^{1,3/2}(\gamma)}.$$

The weak formulation of the fracture model (5.1) reads: Find $p=(p_1,p_2,p_f)\in W$ such that

$$a(p,w) = \sum_{i=1,2}(q_i,w_i)_{\Omega_i} + (q_f,w_f)_\gamma, \quad \forall w=(w_1,w_2,w_f)\in W, \tag{5.5}$$

where $a(\cdot,\cdot): W \times W \mapsto R$

$$
\begin{aligned}
a(p,w) &= \sum_{i=1,2} (\alpha_i^{-1}\nabla p_i, \nabla w_i)_{\Omega_i} + \left(\frac{2}{\alpha_\gamma + \sqrt{\alpha_\gamma^2 + 4\beta_\gamma |\frac{\partial p_f}{\partial y}|}} \frac{\partial p_f}{\partial y}, \frac{\partial w_f}{\partial y} \right)_\gamma \\
&\quad + \sum_{i=1,2} \left(\frac{1}{(2\xi-1)\kappa}(\xi p_i + (1-\xi)p_{i+1} - p_f), w_i \right)_\gamma - \left(\frac{1}{(2\xi-1)\kappa}(p_1 + p_2 - 2p_f), w_f \right)_\gamma .
\end{aligned} \tag{5.6}
$$

The only difference between the forms $a(\cdot,\cdot)$ in (2.6) and (5.6) is the second term. And for the nonlinear system (5.6), it is easy to check that there exist constants c and C satisfying

$$
c \Big| \frac{\partial p_f}{\partial y} \Big|^{3/2}_{L^{3/2}(\gamma)} \le \left(\frac{2}{\alpha_\gamma + \sqrt{\alpha_\gamma^2 + 4\beta_\gamma |\frac{\partial p_f}{\partial y}|}} \frac{\partial p_f}{\partial y}, \frac{\partial p_f}{\partial y} \right)_\gamma \le C \Big| \frac{\partial p_f}{\partial y} \Big|^{3/2}_{L^{3/2}(\gamma)}. \tag{5.7}
$$

The coupled finite element discretization for the fracture model with the nonlinear Darcy-Forchheimer equation in the fracture is proposed.

Algorithm 3. Find $p^h = (p_1^h, p_2^h, p_f^h) \in W^h$ such that

$$
a(p^h, w^h) = \sum_{i=1,2} (q_i, w_i^h)_{\Omega_i} + (q_f, w_f^h)_\gamma, \quad \forall w^h = (w_1^h, w_2^h, w_f^h) \in W^h. \tag{5.8}
$$

And we also study the two-grid algorithm for decoupling this nonlinear problem using a coarse grid approximation in the interface.

Algorithm 4.

1. Solve a coarse grid coupled problem: Find $p^H = (p_1^H, p_2^H, p_f^H) \in W^H$ such that

$$
a(p^H, w^H) = \sum_{i=1,2} (q_i, w_i^H)_{\Omega_i} + (q_f, w_f^H)_\gamma, \quad \forall w^H = (w_1^H, w_2^H, w_f^H) \in W^H. \tag{5.9}
$$

2. Solve a decoupled fine grid problem: Find $\hat{p}^h = (\hat{p}_1^h, \hat{p}_2^h, \hat{p}_f^h) \in W^h$ satisfying for any $w^h = (w_1^h, w_2^h, w_f^h) \in W^h$,

$$
\begin{aligned}
&\sum_{i=1,2} (\alpha_i^{-1}\nabla \hat{p}_i^h, \nabla w_i^h)_{\Omega_i} + \left(\frac{2}{\alpha_\gamma + \sqrt{\alpha_\gamma^2 + 4\beta_\gamma |\frac{\partial \hat{p}_f^h}{\partial y}|}} \frac{\partial \hat{p}_f^h}{\partial y}, \frac{\partial w_f^h}{\partial y} \right)_\gamma \\
&+ \sum_{i=1,2} \frac{\xi}{(2\xi-1)\kappa} \left(\hat{p}_i^h, w_i^h \right)_\gamma + \frac{2}{(2\xi-1)\kappa} \left(\hat{p}_f^h, w_f^h \right)_\gamma \\
= &- \sum_{i=1,2} \frac{(1-\xi)}{(2\xi-1)\kappa} \left(p_{i+1}^H, w_i^h \right)_\gamma + \sum_{i=1,2} \frac{1}{(2\xi-1)\kappa} \left(p_f^H, w_i^h \right)_\gamma \\
&+ \sum_{i=1,2} \frac{1}{(2\xi-1)\kappa} \left(p_i^H, w_f^h \right)_\gamma + \sum_{i=1,2} (q_i, w_i^h)_{\Omega_i} + (q_f, w_f^h)_\gamma.
\end{aligned} \tag{5.10}
$$

Similar to the decoupled method for the linear system (3.4) - (3.5), we can rewrite (5.10) into the following three local problems.

The discrete linear Darcy problem defined in the matrix $\Omega_i, i = 1, 2$:

$$(\alpha_i^{-1}\nabla\hat{p}_i^h, \nabla w_i^h)_{\Omega_i} + \frac{\xi}{(2\xi-1)\kappa}\left(\hat{p}_i^h, w_i^h\right)_\gamma = -\frac{(1-\xi)}{(2\xi-1)\kappa}\left(p_{i+1}^H, w_i^h\right)_\gamma + \frac{1}{(2\xi-1)\kappa}\left(p_f^H, w_i^h\right)_\gamma + (q_i, w_i^h)_{\Omega_i}. \tag{5.11}$$

The discrete nonlinear Darcy-Forchheimer problem defined in the fracture γ:

$$\left(\frac{2}{\alpha_\gamma + \sqrt{\alpha_\gamma^2 + 4\beta_\gamma|\frac{\partial\hat{p}_f^h}{\partial y}|}}\frac{\partial\hat{p}_f^h}{\partial y}, \frac{\partial w_f^h}{\partial y}\right)_\gamma + \frac{2}{(2\xi-1)\kappa}\left(\hat{p}_f^h, w_f^h\right)_\gamma = \sum_{i=1,2}\frac{1}{(2\xi-1)\kappa}\left(p_i^H, w_f^h\right)_\gamma + (q_f, w_f^h)_\gamma. \tag{5.12}$$

From the local problems (5.11) - (5.12), we can see that linear problems are solved in two subdomains Ω_1 and Ω_2, and only the local problem defined in fracture γ is nonlinear, so iteration is required just in the fracture for the Darcy-Forchheimer problem. Hence, the decoupled two-grid algorithm is especially convenient and time-saving for the nonlinear system.

6 Numerical Experiment

We present some numerical examples in this section to verify the accuracy and efficiency of two-grid approach for fracture models. For simplicity, the region for examples is rectangle, $\Omega = [-1, 1]\times[0, 1]$, and $\gamma = \{x = 0\} \times [0, 1]$ is the fracture. The triangulation of Ω is formed by bisecting rectangles of the same shapes. We carry out the following examples with known exact solutions $(\mathbf{u}, p)$ and right-hand side functions and Dirichlet boundary conditions of fracture models are determined by solutions. The finite element spaces are constructed by the linear and constant elements for the pressure p and the velocity $\mathbf{u}$, respectively, and the convergence rates of the H^1 semi-norm of p and the $(L^2)^2$ norm of $\mathbf{u}$ are all expected to be of first-order accuracy for both the coupled method and the two-grid decoupled method with $h = H^{3/2}$.

6.1 Numerical examples for Problem (2.1)

Example 1. The tensors of permeability in the fracture and the surrounding domains are all isotropic and constant, $\mathbf{K}_1 = \mathbf{K}_2 = \mathbf{I}$, $\mathbf{K}_f = 20\mathbf{I}$, where $\mathbf{I}$ is the two dimensional identity matrix. The width of the fracture $d = 0.001$ and $\xi = 4/5$. The fracture permeability is sufficiently large, so the fracture acts as a fast pathway and the flow tends to flow rapidly in the fracture. The analysis solution of Example 1 is given as follows, and error estimates and convergence rates for Algorithms 1 and 2 are shown in Table 1 and 2, respectively.

$$\begin{cases} p_1 = (x+1)sin2\pi y \\ p_2 = -(4x - (1 - 3/(4 * 10^4)))sin2\pi y \\ p_f = sin2\pi y. \end{cases}$$

Table 1

Error estimates and convergence rates for Algorithm 1

h	$\|e^p\|_W$	Rate	$\|e^{\mathbf{u}}\|_{(L^2(\Omega))^2}$	Rate	Time
2^{-2}	0.369767	-	0.367025	-	0.0020s
2^{-3}	0.168760	1.1316	0.183759	0.9994	0.0086s
2^{-4}	0.081184	1.0557	0.091916	0.9998	0.0539s
2^{-5}	0.040128	1.0166	0.045963	0.9999	0.2472s
2^{-6}	0.020004	1.0043	0.022982	1.0000	3.1001s
2^{-7}	0.009995	1.0011	0.011491	1.0000	53.9027s
2^{-8}	0.004996	1.0002	0.005745	1.0000	1120.0023s
2^{-9}	0.002498	1.0001	0.002872	1.0000	19317.8788s

Table 2

Error estimates and convergence rates for Algorithm 2

$h = H^{3/2}$	H	$\|e^p\|_W$	Rate	$\|e^{\mathbf{u}}\|_{(L^2(\Omega))^2}$	Rate	Time
2^{-3}	2^{-2}	0.196694	-	0.196704	-	0.0082s
2^{-6}	2^{-4}	0.024248	3.0200	0.024251	3.0200	2.9547s
2^{-9}	2^{-6}	0.002988	3.0206	0.002993	3.0183	11076.0313s

Example 2. $\mathbf{K}_1 = \mathbf{K}_2 = 10\mathbf{I}$, and $\mathbf{K}_f = 10^{-3}\mathbf{I}$, $d = 0.001$ and $\xi = 4/5$. In this case, the fracture permeability is much smaller than the surrounding matrix permeability, so the fluid barely flows through the fracture and the fracture can be seen as geologic barrier. The results are presented in the following two tables.

$$\begin{cases} p_1 = (x+1)sin2\pi y \\ p_2 = -(3x+9)sin2\pi y \\ p_f = 2sin2\pi y. \end{cases}$$

Table 3

Error estimates and convergence rates for Algorithm 1

h	$\|e^p\|_W$	Rate	$\|e^{\mathbf{u}}\|_{(L^2(\Omega))^2}$	Rate	Time
2^{-2}	0.349013	-	0.282293	-	0.3052s
2^{-3}	0.140336	1.3143	0.134201	1.0727	0.4499s
2^{-4}	0.066227	1.0834	0.066245	1.0185	0.9464s
2^{-5}	0.032590	1.0229	0.033018	1.0045	2.8728s
2^{-6}	0.016227	1.0060	0.016496	1.0011	11.8176s
2^{-7}	0.008105	1.0015	0.008246	1.0003	79.12588s
2^{-8}	0.004051	1.0003	0.004123	1.0001	1070.7029s
2^{-9}	0.002025	1.0001	0.002061	1.0000	15456.3896s

Table 4

Error estimates and convergence rates for Algorithm 2

$h = H^{3/2}$	H	$\|e^p\|_W$	Rate	$\|e^{\mathbf{u}}\|_{(L^2(\Omega))^2}$	Rate	Time
2^{-3}	2^{-2}	0.141561	-	0.134517	-	0.0106s
2^{-6}	2^{-4}	0.016260	3.1220	0.016501	3.0271	1.6215s
2^{-9}	2^{-6}	0.002026	3.0046	0.002061	3.0008	8360.2546s

Example 3. We test an example with anisotropic fracture permeability,

$$\mathbf{K}_1 = \mathbf{K}_2 = 10\mathbf{I}, \quad \text{and} \quad \mathbf{K}_f = \begin{pmatrix} 10 & 0 \\ 0 & 10^{-3} \end{pmatrix}.$$

The width of the fracture is $d = 10^{-3}$, and $\xi = 2/3$.

$$\begin{cases} p_1 = (x+1)sin2\pi y \\ p_2 = -(2x+4)sin2\pi y \\ p_f = sin2\pi y. \end{cases}$$

Table 5

Error estimates and convergence rates for Algorithm 1

h	$\|e^p\|_W$	Rate	$\|e^{\mathbf{u}}\|_{(L^2(\Omega))^2}$	Rate	Time
2^{-2}	0.320980	-	0.283537	-	0.0020s
2^{-3}	0.137929	1.2186	0.135265	1.0677	0.0075s
2^{-4}	0.066287	1.0571	0.066827	1.0173	0.0261s
2^{-5}	0.032781	1.0158	0.033315	1.0042	0.2222s
2^{-6}	0.016343	1.0041	0.016645	1.0010	3.1018s
2^{-7}	0.008166	1.0010	0.008321	1.0002	54.1243s
2^{-8}	0.004082	1.0002	0.004160	1.0001	1138.9655s
2^{-9}	0.002041	1.0001	0.002080	1.0000	17615.2500s

Table 6

Error estimates and convergence rates for Algorithm 2

$h = H^{3/2}$	H	$\|e^p\|_W$	Rate	$\|e^{\mathbf{u}}\|_{(L^2(\Omega))^2}$	Rate	Time
2^{-3}	2^{-2}	0.139436	-	0.135683	-	0.0083s
2^{-6}	2^{-4}	0.016382	3.0894	0.016655	3.0262	2.7181s
2^{-9}	2^{-6}	0.002041	3.0042	0.002089	2.9946	10125.3466s

In above tables, we list errors between the exact solutions and the finite element solutions of the coupled method and decoupled two-grid algorithm. The second table of every example shows that the convergence rates of the H^1 semi-norm of p and the $(L^2)^2$ norm of $\mathbf{u}$ still hold first-order reduction, which is consistent with our analysis. And by comparing the first table and the second table of every example, the two-grid decoupled algorithm maintains the same order accuracy as the coupled method. In the above three linear experiments, the Gauss-Seidel iteration is used to solve the algebraic systems about the pressure and the computing times for iterations are also shown in tables. A comparison of two algorithms, one can easy see that the computation time of decoupled method is almost reduced by half, even though a coupled solver is required in the coarse grids. And if the parallel process is applied to the two-grid algorithm, it will be more efficient and save more time.

6.2 Numerical examples for Problem (5.1)

We also use linear and constant elements to approximate the pressure and velocity of the fracture model with Darcy-Forchheimer equation in the fracture. In order to show the two-grid approximation accuracy and efficiency, both coupled method Algorithm 3 and decoupled method Algorithm 4 are complemented by the Picard iteration algorithm with zero initial guess for the nonlinear system in the fracture. For Algorithm 3, we need do the iteration in the whole domain and the stopping criterion is $\|P^{m+1} - P^m\|_{L^2(\Omega)} \leq 10^{-8}$, where P^m is the nodal-value vector of the pressure for the mth iterate, while for the two-grid decoupled method Algorithm 4, the Picard iteration is just used for pressure in the fracture γ and the stopping criterion is $\|P_f^{m+1} - P_f^m\|_{L^2(\gamma)} \leq 10^{-8}$. For simplicity, we take $\alpha_i = \mathbf{I}$, $\alpha_\gamma = \beta_\gamma = 1$, $\kappa = 1$ and $\xi = \frac{4}{5}$. The exact solution is described as follows and error estimates is shown in the following tables.

$$\begin{cases} p_1 = (x+1)sin2\pi y, \\ p_2 = -(4x+2)sin2\pi y, \\ p_f = sin2\pi y. \end{cases}$$

$$\mathbf{u}_1 = -\begin{pmatrix} sin2\pi y \\ 2\pi(x+1)cos2\pi y \end{pmatrix}, \quad u_f = -2\pi cos2\pi y, \quad \text{and} \quad \mathbf{u}_2 = -\begin{pmatrix} 4sin2\pi y \\ 2\pi(4x+2)cos2\pi y \end{pmatrix}.$$

And the right-hand side functions

$$\begin{cases} q_1 = 4\pi^2(x+1)sin2\pi y, & \text{in } \Omega_1, \\ q_2 = -4\pi^2(4x+2)sin2\pi y, & \text{in } \Omega_2 \\ q_f = (4\pi^2+5)sin2\pi y, & \text{in } \gamma, \\ g = -4\pi^2|cos2\pi y|cos2\pi y, & \text{in } \gamma. \end{cases}$$

Table 7

Error estimates and convergence rates for Algorithm 3

h	$\|e^p\|_W$	Rate	$\|e^{\mathbf{u}}\|_{(L^2(\Omega))^2}$	Rate	Time
2^{-2}	0.414460	-	0.287813	-	0.0540s
2^{-3}	0.159646	1.3764	0.139340	1.0465	0.0778s
2^{-4}	0.071645	1.1559	0.069033	1.0132	0.0847s
2^{-5}	0.034764	1.0432	0.034435	1.0034	0.2743s
2^{-6}	0.017248	1.0112	0.017207	1.0009	1.0933s
2^{-7}	0.008607	1.0028	0.008602	1.0002	5.3310s
2^{-8}	0.004301	1.0007	0.004301	1.0001	29.7199s
2^{-9}	0.002150	1.0001	0.002150	1.0000	173.9807s

Table 8

Error estimates and convergence rates for Algorithm 4

$h = H^{3/2}$	H	$\|e^p\|_W$	Rate	$\|e^{\mathbf{u}}\|_{(L^2(\Omega))^2}$	Rate	Time
2^{-3}	2^{-2}	0.165276	-	0.140696	-	0.0703s
2^{-6}	2^{-4}	0.017647	3.2274	0.017366	3.0182	0.1645s
2^{-9}	2^{-6}	0.002161	3.0298	0.002156	3.0101	7.2832s

For the nonlinear experiment, the two-grid decoupled algorithm still holds the same order accuracy as the coupled method for errors of the H^1 semi-norm of p and the $(L^2)^2$ norm of $\mathbf{u}$. We directly solve the algebraic system for the nonlinear problem, and since the Picard iterations are needed just in the fracture instead of the whole domain, the computation time is greatly reduced.

The proposed theory and experiments suggest that the fracture model can efficiently be decoupled by a coarse grid approximation to the interface. This allows us to solve local problems independently, and we can even solve them by different process, which reduces time consuming greatly, especially for the nonlinear system.

References

[1] C. Alboin, J. Jaffre, J. Roberts, and C. Serres, Domain decomposition for flow in fractured porous media, Domain Decomposition Methods in Sciences and Engineering, 1999, pp. 365-373.

[2] V. Martin, J. Jaffre, and J. Roberts, Modeling fractures and barriers as interfaces for flow in porous media, SIAM J. Sci. Comput., 26(2005), pp. 1667-1691.

[3] P. Angot, F. Boyer, and F. Hubert, Asymptotic and numerical modelling of flows in fractured porous media, Mathematical Modelling and Numerical Analysis, 43(2009), pp. 239-275.

[4] F. Morales, and R. Showalter, The narrow fracture approximation by channeled flow, Journal of Mathematical Analysis and Applications, 365(2010), pp. 320-331.

[5] N. Frih, V. Martin, J. Roberts, and A. Saada, Modeling fractures as interfaces with nonmatching grids, Computational Geosciences, (16)2012, pp. 1043-1060.

[6] M. Lesinigo, C. DAngelo, and A. Quarteroni, A multiscale DarcyCBrinkman model for fluid flow in fractured porous media, Numerische Mathematik, 117(2011), pp. 717-752.

[7] P. Forchheimer, Wasserbewegung durch boden, Zeitz. Ver. Duetch Ing., 45(1901), pp. 1782-1788.

[8] H. Rui, and H. Pan, A Block-Centered Finite Difference Method for the Darcy–Forchheimer Model, SIAM Journal on Numerical Analysis, 50(2012), pp. 2612-2631.

[9] N. Frih, J. Roberts, and A. Saada, Modeling fractures as interface: a model for forchheimer fracture, Comput. Geosci., 12(2008), pp. 91-104.

[10] P. Knabner, and J. Roberts, Mathmatical analysis of a discrete fracture model coupling Darcy flow in the matrix with Darcy-Forchheimer flow in the fracture, ESAIM: Mathematical modelling and Numerical Analysis, 48(2014), pp. 1451-1472.

[11] A. Quarteroni, and A. Valli, Domain decomposition methods for partial differential equations, Oxford University Press, 1999.

[12] R. Glowinski, T. Pan, and T. Hesla, A distributed Lagrange multiplier/fictitious domain method for particulate flows, International Journal of Multiphase Flow, 25(1999), pp. 755-794.

[13] J. Xu, A novel two-grid method for semilinear elliptic equations, SIAM Journal on Scientific Computing, 15(1994), pp. 231-237.

[14] J. Xu, Two-grid discretization techniques for linear and nonlinear PDEs, SIAM Journal on Numerical Analysis, 33(1996), pp. 1759-1777.

[15] M Mu, and J, Xu, A two-grid method of a mixed Stokes-Darcy model for coupling fluid flow with porous media flow, SIAM Journal on numerical analysis, 45(2007), pp. 1801-1813.

[16] M. Cai, M. Mu, and J. Xu, Numerical solution to a mixed Navier-Stokes/Darcy model by the two-grid approach, SIAM Journal on Numerical Analysis, 47(2009), pp. 3325-3338.

[17] M, Marion, and J. Xu, Error estimates on a new nonlinear Galerkin method based on two-grid finite elements, SIAM Journal on Numerical Analysis, 32(1995), pp. 1170-1184.

[18] J. Xu, Iterative methods by space decomposition and subspace correction, SIAM review, 34(1992), pp. 581-613.

[19] H. Rui, and W. Liu, A Two-Grid Block-Centered Finite Difference Method For Darcy–Forchheimer Flow in Porous Media, SIAM Journal on Numerical Analysis, 53(2015), pp. 1941-1962.

[20] F. Brezzi, and M. Fortin, Mixed and hybrid finite element methods, Springer-Verlag, New York, 1991.

[21] H. Pan, and H. Rui, Mixed element method for two-dimensional Darcy-Forchheimer model, Journal of Scientific Computing, 52(2012), pp. 563-587.